Titrating synapse number to treat MDD in Fragile X Syndrome

Chelcie F. Heaney[1,2], Sanjeev V. Namjoshi[1], Ayse Uneri[1], Eva C. Bach[1,2], Jeffrey L. Weiner[1,2], Kimberly F. Raab-Graham[1,2*].

Affiliations:

[1]Department of Physiology and Pharmacology, Wake Forest University Health Sciences, Medical Center Boulevard, Winston-Salem, NC 27157, USA

[2] Wake Forest Translational Alcohol Research Center (WF-TARC), Wake Forest University Health Sciences, Medical Center Boulevard, Winston-Salem, NC 27157, USA

*Correspondence to: kraabgra@wakehealth.edu.

Competing interests: The authors declare no competing interests.

Abstract:

Rapid antidepressants are novel treatments for major depressive disorder (MDD) and work by blocking N-methyl-aspartate receptors (NMDAR), which, in turn, activate the protein synthesis pathway regulated by mechanistic/mammalian target of rapamycin complex 1 (mTORC1). Our recent work demonstrates that the RNA-binding protein Fragile X Mental Retardation Protein (FMRP) is downregulated in dendrites upon treatment with a rapid antidepressant. Here, we show that the behavioral effects of the rapid antidepressant Ro-25-6981 require FMRP expression and Ro-25-6981 treatment promotes differential mRNA binding to FMRP in an mTORC1-dependent manner. Further, we identified that these mRNAs regulate transsynaptic signaling. Using a novel technique, we show that synapse formation underlying the behavioral effects of Ro-25-6981 require $GABA_BR$-mediated mTORC1 activity in WT animals. Finally, we demonstrate that in a clinically relevant animal model of Fragile X Syndrome (FXS), which lacks FMRP expression, $GABA_BR$ activity is detrimental to the effects of Ro-25-6981. These effects are rescued when $GABA_BRs$ are blocked in addition to treatment with Ro-25-6981, indicating that rapid antidepressants alone may not be an effective treatment for people with FXS and MDD.

Introduction

Over the past 50 years, treatment for major depressive disorder (MDD) has been limited[1], with selective serotonin reuptake inhibitors (SSRIs) as the most commonly prescribed treatment for the general population. Recently, MDD treatment entered a new era with the discovery that glutamate N-methyl-D-aspartate receptor (NMDAR) antagonists produce antidepressant-like effects[2], perhaps by blocking NMDARs containing the 2B subunit (GluN2B)[3]. Importantly, these drugs have a rapid onset and work in a treatment-resistant population, with relief of MDD symptoms within hours of a single infusion that can last up to a week[4-6]. Thus, NMDAR antagonists are considered paradigm-shifting treatments for MDD[7].

Activation of mechanistic/mammalian target of rapamycin complex 1 (mTORC1), a serine-threonine kinase that regulates protein synthesis and promotes new synapse formation, is key to reducing MDD symptoms through NMDAR antagonism[8]. mTORC1 regulates protein synthesis in dendrites by utilizing mRNAs that are targeted and translated in a site-specific and temporal fashion. The coordinated expression of these mRNAs that code for proteins involved in synaptic and structural plasticity[9,10] may be regulated by RNA-binding proteins (RBPs). Our recent work suggests that NMDAR antagonism rapidly downregulates dendritic expression of the RBP Fragile X Mental Retardation Protein (FMRP)[11].

FMRP is one of the best characterized RBPs, affecting mRNA trafficking[12], mRNA repression in dendrites[13], as well as being implicated in Fragile X Syndrome (FXS), the leading single-gene cause of autism spectrum disorder (ASD)[14,15]. Loss-of-function mutations in the FMR1 gene, which codes for FMRP[16], lead to FXS. Notably,

54 people who are FMR1 premutation carriers exhibit higher rates of MDD and depressed
55 mood compared to the general population[17-19]. Additionally, people with ASD have an
56 increased risk of developing MDD by the time they are 30 years old compared to people
57 without ASD[20]. Moreover, caretakers of people with FXS identify mood and depression
58 as a priority for treatment development[21]. While FMRP is extensively characterized in
59 the context of ASD, its role in MDD and MDD treatments is unclear. For instance,
60 research indicates that SSRIs are ineffective in an animal model of FXS[23], suggesting
61 that people with FXS and MDD may be treatment-resistant to traditional MDD
62 pharmacotherapies.

63 In light of these data, critical questions need to be addressed: (1) is FMRP
64 required for the rapid antidepressant properties of NMDAR antagonists, (2) given the
65 importance of mTORC1 signaling in rapid antidepressant efficacy, do mTORC1 and
66 FMRP regulate specific cellular functions, and (3) are rapid antidepressants an effective
67 treatment for MDD in FXS?

68 Herein, we demonstrate that transsynaptic signaling and presynaptic
69 engagement are mTORC1-dependent and are required for new synapse formation.
70 Further, these mechanisms underlying the rapid antidepressant efficacy of the GluN2B-
71 specific antagonist Ro-25-6981, require activity-dependent FMRP expression.
72 Moreover, we demonstrate that, unlike wild-type (WT) mice, treatment with Ro-25-6981
73 alone is insufficient to promote new synapse formation or antidepressant-like effects on
74 behavior in *Fmr1* knockout (KO) mice, similar to SSRIs[23]. Finally, we provide data that
75 γ-aminobutyric acid B receptor ($GABA_BR$) signaling prevents the actions of Ro-25-6981
76 in *Fmr1* KO mice. Blocking $GABA_BRs$ with the specific antagonist CGP35348 restores

77 the antidepressant-like effect on behavior and increases synapse number when
78 coadministered with Ro-25-6981 in *Fmr1* KO mice. Importantly, our findings propose a
79 new combination therapy effective to treat MDD in FXS.
80

81 **Materials and Methods**

82 *Detailed Materials and Methods are outlined in the Supplement.*

83 Animals

84 Male and female WT (C57BL/6, Jackson Laboratory) and *Fmr1* KO (B.6129P2-
85 Fmr1tm1Cgr/J, Jackson Laboratory) mice between the ages of 2-5 months were used.
86 All animals were randomly assigned to treatment groups. We found no significant effect
87 of sex or sex X treatment interaction (data presented in Supplement). All experiments
88 were carried out in accordance with the National Institutes of Health's Guide for the
89 Care and Use of Laboratory Animals and approved by the Wake Forest Institutional
90 Animal Care and Use Committee (IACUC).
91

92 Pharmacology

93 For behavioral and *in vivo* experiments, animals received intraperitoneal (i.p.) injections
94 of Ro-25-6981 (10 mg/kg, Tocris 1594) with or without CGP35348 (100 mg/kg; Tocris,
95 1245), or 0.9% physiological saline vehicle (0.01 ml/g, LabChem). Animals in the RIP-
96 Seq experiment received either Ro-25-6981 (10 mg/kg) with or without rapamycin (6
97 mg/kg; LC Laboratories, #R-5000), or 0.9% physiological saline (200 µl). For *in vitro*
98 experiments, Ro-25-6981 (10 µM), rapamycin (200 nM), and baclofen (50 µM; Tocris,

99 #0796) were used. Vehicle control cells were treated with water (vehicle for Ro-25-6981
100 and baclofen) and/or 0.1% DMSO (vehicle for rapamycin).
101
102 Forced swim test
103 Animals were placed into a glass cylinder filled with water 23-25ºC for six minutes;
104 animals were quickly removed at the end, dried, and returned to their warmed home
105 cage. Each animal was run in two FST sessions (see Fig. 1A for timeline); the first
106 session acutely stressed the animals, and the second session, 24 hours after the first,
107 was video recorded and scored for immobility in the last four minutes using Ethovision
108 (version 11.5, Noldus).
109
110 Splash test
111 Animals were individually assessed in their home cage by applying 200 µl of 10%
112 sucrose to their dorsal coat. Animals were video-recorded for five minutes and later
113 scored for grooming behavior (licking, grooming with forepaws, and scratching).
114
115 RNA Immunoprecipitation (RIP)
116 Animals were sacrificed 45 minutes after drug administration, and whole cortices were
117 rapidly dissected out and flash frozen on dry ice. RIP-Seq was modified from previous
118 methods shown to significantly reduce background mRNA binding[24,25].
119
120 Immunoblotting

121 Animals were sacrificed 45 minutes after drug administration, and cortices were
122 processed according to previously published methods[11,26-28].
123
124 Immunohistochemistry and *in vivo* proximity ligation assay
125 Animals were deeply anesthetized 45 minutes after drug administration and underwent
126 transcardial perfusion. Brains were sectioned 25 µm thick on a Leica SM2010F sliding
127 microtome and put into cryoprotectant. Slices were permeabilized and blocked prior to
128 overnight primary antibody incubation at 4ºC. Slices underwent a two-hour incubation at
129 37ºC in secondary antibodies, then incubated in ligase for 30 minutes at 37ºC. Finally,
130 slices underwent the amplification/polymerase step for two hours at 37ºC.
131
132 Cell culture and *in vitro* proximity ligation assay (PLA)
133 Primary neuronal hippocampal cultures were prepared from postnatal day 0-3 mouse
134 pups from WT or *Fmr1* KO mice according to previously published methods[11,26-28]. Cells
135 were plated between 70-100,000 per 12 mm on glass coverslips. Neuronal cultures
136 were used at 18-21 days *in vitro*. Drug treatments were done in media. Fixed neurons
137 were blocked and permeabilized and then incubated with primary antibodies for one
138 hour at RT, followed by secondary antibody incubation for one hour at RT
139 (immunofluorescence) or 37°C (PLA). PLA coverslips were then incubated with ligation
140 solution for 30 minutes at 37°C, followed by incubation in amplification/polymerase
141 buffer for 100 minutes at 37°C.
142
143 Microscopy and analysis

144 All images within a given experiment were acquired and analyzed using the same
145 settings. All images were acquired on a Nikon A1plus confocal microscope and
146 analyzed with Nikon NIS-Elements AR (version 4.40.00).
147
148 Statistical Analyses
149 Prism (version 7.05, GraphPad) was used for all statistical analyses. Statistical
150 comparisons were made using Student's t-test, one-way analysis of variance (ANOVA),
151 or two-way ANOVA where appropriate. Newman-Keuls post-hoc tests were performed
152 in the event of significant ANOVAs. Outliers were determined using Grubbs' test
153 (α=0.05). All data are expressed as mean ± standard error of the mean (SEM).
154
155 **Results**
156 ***The rapid antidepressant behavioral effects of Ro-25-6981 require FMRP***
157 ***expression***
158 We recently showed that dendritic FMRP expression is rapidly reduced in WT
159 dendrites after treatment with the GluN2B-specific antagonist Ro-25-6981, suggesting
160 that activity-dependent expression of FMRP and FMRP-dependent translation in
161 dendrites may be necessary for antidepressant efficacy[11]. To test this hypothesis, we
162 treated acutely stressed WT and *Fmr1* KO mice with a single i.p. injection of Ro-25-
163 6981 (see Fig. 1A for timeline). We then analyzed performance in two well-
164 characterized behavioral tasks that measure antidepressant efficacy – the forced swim
165 test (FST), a measure of behavioral despair, and the splash test, a measure of
166 motivated self-care[2,29-32]. Consistent with our previous results[26,27], Ro-25-6981-treated

167 WT animals are mobile about 60s more in the FST (Fig. 1B) and groom about twice as
168 frequently in the splash test (Fig. 1C), indicative of an antidepressant-like effect.
169 However, Ro-25-6981 does not affect performance in either task when administered to
170 *Fmr1* KO mice. Together, these results confirm our hypothesis that the RBP FMRP is
171 required for the behavioral effects of rapid antidepressants.
172

173 ***mTORC1-sensitive FMRP-target mRNAs are regulated by Ro-25-6981 treatment***

174 We next set out to identify the FMRP-target mRNAs that are regulated by Ro-25-
175 6981, and which may underlie its antidepressant efficacy. We treated WT and *Fmr1* KO
176 mice with Ro-25-6981 and collected brains 45 minutes post-administration, a time point
177 at which behavioral changes[26] and mTORC1 activation are observed[2]. Cortices were
178 processed for RNA immunoprecipitation (RIP), followed by RNASeq (RIP-Seq), using a
179 specific antibody against FMRP[33] (see Supplemental Methods, Fig. S1-S4, and Tables
180 S1-S3 for RIP-Seq data preprocessing, filtering, quality control, and processing). As a
181 control for nonspecific binding, FMRP-RIP was performed, in parallel, on *Fmr1* KO
182 cortices. Ro-25-6981 treatment promoted the differential binding of 283 transcripts to
183 FMRP relative to control (Fig 2A; light blue circle). These data indicate that FMRP
184 regulates the availability of mRNAs for translation in response to Ro-25-6981 treatment.

185 We and others show that rapid antidepressants, including Ro-25-6981, increase
186 mTORC1-dependent synthesis of several synaptic proteins necessary for its
187 antidepressant effects[2,26,27]. To identify the mTORC1-sensitive transcripts among the
188 283 FMRP-target mRNAs we identified, we performed RIP-Seq on cortices from mice
189 co-injected with Ro-25-6981 plus the mTORC1 inhibitor rapamycin. We then compared

190 the differentially regulated FMRP-target mRNAs that are sensitive to both Ro-25-681
191 treatment (Fig. 2A, light blue circle) and mTORC1 activity (Fig. 2A, light red circle).
192 Differential gene expression analysis between these two treatments revealed 190
193 overlapping transcripts (false discovery rate cutoff of 0.1; Fig. 2A, 2B; Table S4, S5[34]).
194 Of these overlapping FMRP-target mRNAs sensitive to Ro-25-6981 treatment and
195 mTORC1 activity, 99.5% change in the same direction (58.9% upregulated/released,
196 40.5% downregulated/bound). FMRP is best known for repressing mRNA translation[35],
197 and we expected that treatment with Ro-25-6981 would induce FMRP to release select
198 transcripts to be translated (~59% are released/upregulated). We were surprised to find
199 that FMRP also bound a new set of target mRNAs (~41% become
200 bound/downregulated). Interestingly, we identified *Fmr1* mRNA as one of the mTORC1-
201 sensitive mRNA targets bound to FMRP after Ro-25-6981 treatment. These data
202 indicate that FMRP represses its own mRNA translation in a Ro-25-6981/mTORC1-
203 dependent manner (Fig. 2C, Table S5). We verified *Fmr1* as a downregulated target by
204 analyzing FMRP expression *in vivo* 45 minutes after treatment. As expected, and in line
205 with our previous results[11], we found that mice treated with Ro-25-6981 express
206 significantly less FMRP in cortical lysates by Western blot analysis (Fig. 2D) and in the
207 CA1 stratum radiatum by immunofluorescence (Fig. 2E, 2F). Together, these data
208 verify our RIP-Seq results and suggest that Ro-25-6981 regulates the dynamic
209 expression of FMRP.
210
211 ***FMRP-target mRNAs regulate transsynaptic signaling***

212 Next, we used gene ontology (GO), a method of clustering transcripts based on
213 their coordinated biological processes, to identify critical mechanisms mediated by Ro-
214 25-6981/mTORC1/FMRP (Fig. 3A, 3B). Interestingly, these analyses revealed
215 transsynaptic signaling to be the most significantly enriched GO cluster in both
216 conditions (Fig. 3A, control/Ro; Fig. 3B, Ro+Rapa/Ro). Importantly, of the 190 Ro-25-
217 6981/mTORC1-sensitive FMRP target mRNAs (Fig. 2A), ~60% are transsynaptic (Fig.
218 3C, *upper right quadrant*, Fig. S4D, Table S5). These analyses suggest that regulating
219 transsynaptic signaling is a specific role for the FMRP-target mRNAs that are sensitive
220 to both mTORC1 activity and Ro-25-6981 treatment.
221

222 ***Transsynaptic signaling requires both NMDAR blockade and $GABA_BR$-mediated***
223 ***mTORC1 activation***

224 Transsynaptic signaling facilitates the coordinated communication of pre- and
225 postsynaptic terminals[36]. Additionally, new synapse formation is suggested to underlie
226 rapid antidepressant efficacy[2]. We have previously shown that activation of traditionally
227 inhibitory $GABA_BRs$ in the presence of an NMDAR antagonist unexpectedly increases
228 L-type calcium channel activity, which thereby increases dendritic mTORC1 activation
229 and downstream protein synthesis[26,27]. To validate that Ro-25-6981 affects
230 transsynaptic signaling, we capitalized on the ability to tightly control mTORC1 activity
231 in the cell culture system. We measured the expression of postsynaptic density 95
232 (PSD-95) and synapsin-1, two prototypical synaptic proteins that specifically localize to
233 post- and presynaptic terminals, respectively[2,33]. Notably, both NMDAR antagonism and
234 $GABA_BR$ activity are required to activate mTORC1[26]. Thus, we treated cultured primary

235 hippocampal neurons (see Fig. 4A for timeline) with Ro-25-6981 (no mTORC1 activity *in*
236 *vitro*), Ro-25-6981 with the $GABA_B$ agonist baclofen (mTORC1 activity *in vitro*), or Ro-
237 25-6981 with baclofen and the mTORC1 inhibitor rapamycin (mTORC1 blocked *in vitro*).
238 We found that GluN2B-specific antagonism increased expression of the postsynaptic
239 marker PSD-95 in an mTORC1-independent manner (Fig. 4B, 4C). In contrast,
240 expression of the presynaptic marker synapsin-1 increased only in the neurons with
241 mTORC1 activity (Ro-25-6981+Baclofen; Fig. 4B, 4D). When we measured
242 colocalization of PSD-95 with synapsin-1, however, we did not find a significant effect of
243 treatment (Fig. 4E), likely due to these proteins being juxtaposed versus overlapping.
244 Realizing the limitations of colocalization as a correlate of synapse number, we
245 developed a fluorescent assay that could detect pre- and postsynaptic engagement,
246 and, thus, indicate new synapse formation. Noting that array tomography studies
247 demonstrate that postsynaptic PSD-95 and presynaptic synapsin-1 localize within 40
248 nm of each other[37], we surmised we could utilize a proximity ligation assay (PLA) to
249 detect protein-protein interactions between proximal pre- and postsynaptic proteins
250 located across the synaptic cleft within 0-40 nm. Consistent with our immunostaining
251 data, NMDAR antagonism alone (Ro-25-6981) did not increase synapse formation, as
252 indicated by no change in PLA puncta number relative to control (Fig. 4F, 4G).
253 However, when we activated mTORC1 (Ro-25-6981+baclofen), the number of
254 detectable PLA puncta in dendrites increased by ~ 65% (Fig. 4F, 4G). Further, when we
255 inhibited mTORC1 with rapamycin (Ro-25-6981+Rapa+Bac), the number of detected
256 synapses decreased back to baseline (Fig. 4F, 4G). Thus, $GABA_BR$-mediated mTORC1

257 activation is required for presynaptic engagement for synapse formation with Ro-25-
258 6981.

259 We next verified that the change in synapse number detected *in vitro* is reflected
260 *in vivo*. Because there are few inhibitory neurons in hippocampal cultures[38,39], baclofen
261 is necessary to activate $GABA_B$Rs *in vitro*. However, *in vivo* ketamine or Ro-25-6981
262 treatment is sufficient to increase release of endogenous GABA[40] and to promote
263 mTORC1 activity and antidepressant-like effects on behavior[26,27]. Therefore, we
264 inhibited $GABA_B$Rs in order to investigate the effects of $GABA_B$R-mediated mTORC1
265 activity *in vivo*. Thus, we treated WT mice with Ro-25-6981 or Ro-25-6981 and the
266 specific $GABA_B$R antagonist CGP35348 to block $GABA_B$R signaling and downstream
267 mTORC1 activation[26]. Indeed, consistent with our *in vitro* PLA results, we found that Ro-
268 25-6981 treatment increased the number of detected synapses and that inhibiting
269 mTORC1 activity with CGP35348 prevented this increase (Fig. 4H).

270

271 ***$GABA_B$R activity is detrimental to synapse formation and rapid antidepressant***
272 ***efficacy of Ro-25-6981 in a preclinical mouse model of FXS***

273 Next, we sought to validate the requirement of FMRP expression for mTORC1-
274 dependent synapse formation upon treatment with Ro-25-6981. We replicated the PLA-
275 synapse assay in hippocampal slices from *Fmr1* KO mice. We predicted that if the
276 activity-dependent release of FMRP-target mRNAs is required for mTORC1-dependent
277 transsynaptic signaling and synapse formation, then the relative increase in synapses
278 detected by PLA upon treatment will be absent in the *Fmr1* KO mouse. Surprisingly, we
279 instead found a significant decrease of about 43% in the number of detected synapses

280 in *Fmr1* KO mice treated with Ro-25-6981 (Fig. 5A, 5B). Further, treatment with Ro-25-
281 6981 and CGP35348 unexpectedly reversed this decrease and significantly increased
282 the number of detected synapses by about 47% compared to control animals (Fig. 5A,
283 5B). These data suggest that in the presence of FMRP expression, $GABA_BR$ signaling
284 is required for rapid antidepressant-mediated synaptogenesis; however, when FMRP
285 expression is absent, $GABA_BR$ signaling is detrimental and needs to be blocked for
286 synaptogenesis to occur.

287 If the increase in synapses in WT animals underlies the efficacy of Ro-25-6981
288 as a rapid antidepressant, we thus questioned whether blocking $GABA_BR$ activity in
289 conjunction with Ro-25-6981 treatment would promote an antidepressant-like effect on
290 behavior in *Fmr1* KO animals. We tested this hypothesis by examining the effect of Ro-
291 25-6981 with or without the $GABA_BR$ antagonist CGP35348 on behavior of *Fmr1* KO
292 mice in the FST and splash test (see Fig. 1A for timeline). Indeed, *Fmr1* KO animals
293 treated with Ro-25-6981+CGP35348 decreased immobility in the FST by about 80s
294 (Fig. 5C) and increased grooming frequency in the splash test by about seven times
295 compared to control KO animals (Fig. 5D). Importantly, CGP35348 alone does not
296 affect *Fmr1* KO mice in the FST[11] or splash test (Fig. S5). Thus, our data indicate that
297 the rapid antidepressant efficacy of Ro-25-6981 requires FMRP expression, and
298 treatment with Ro-25-6981 regulates mTORC1/FMRP-target mRNAs that promote
299 transsynaptic signaling and synaptogenesis. However, in cases where FMRP
300 expression is absent, as in *Fmr1* KO animals, Ro-25-6981 is ineffective as a rapid
301 antidepressant. Only when $GABA_BR$ activity is blocked in these animals does Ro-25-
302 6981 increase synaptogenesis and promote antidepressant-like effects.

303

304 **Discussion**

305 Previously, we discovered that the molecular mechanism underlying the
306 behavioral efficacy of rapid antidepressants requires $GABA_BR$-mediated mTORC1
307 activity (Fig. 5E)[11,26,27]. Here, we demonstrate that rapid antidepressants regulate
308 mTORC1-sensitive FMRP-target mRNAs that are involved in transsynaptic signaling.
309 Further, we show, with our newly developed assay, that rapid antidepressant treatment
310 in conjunction with $GABA_BR$ activity promotes synaptogenesis *in vitro* and *in vivo* in WT
311 animals. In *Fmr1* KO animals, $GABA_BR$ activity appears to prevent the beneficial effects
312 of rapid antidepressants. However, blocking $GABA_BRs$ rescued these detrimental
313 effects in *Frm1* KO mice and promoted the rapid antidepressant effects similar to what
314 we see in WT animals.

315 Importantly, our report is the first to provide a promising antidepressant therapy
316 for people with FXS. Using a clinically relevant animal model of FXS, we show that,
317 opposite to the effects observed in WT animals, reducing $GABA_BR$ activity may promote
318 antidepressant efficacy[11,26,27]. While clinical trials demonstrate that treatment with the
319 $GABA_B$ agonist baclofen improves irritability and social responsiveness in people with
320 FXS and ASD, these results are mixed[41-43]. Additionally, baclofen can cause adverse
321 side effects, including hyperactivity and anxiety[44-46]. These data, in light of our results,
322 raise the question as to why $GABA_BR$ signaling is required for synaptogenesis and
323 antidepressant efficacy in WT mice, yet prohibitive in *Fmr1* KO mice. One clue comes
324 from our previous data demonstrating that traditional inhibitory postsynaptic $GABA_BR$-
325 GIRK signaling is absent in *Fmr1* KO dendrites, and may be constitutively excitatory

326 instead[11]. By blocking $GABA_BR$ activity, we may be preventing excessive excitation[47]
327 and the synapse reduction seen in Ro-25-6981-only treated *Fmr1* KO mice (Fig. 5A and
328 5B). Further, these data indicate that treating MDD in people with FXS or an FMR1
329 premutation may require combination therapy, as traditional[23] and rapid antidepressants
330 alone (as reported here) are not effective in animal models of FXS. A recent clinical
331 report indicates that oral rapamycin treatment prior to ketamine prolongs the
332 antidepressant effects of ketamine in a treatment-resistant population[48]. Although the
333 underlying causes of treatment-resistance are unclear, all together, these data support
334 the idea that rapid antidepressants in combination with other drugs that modify
335 mTORC1 activity, such as we show with CGP35348, may be more effective in select
336 populations.

337 Importantly, this study provides timely data regarding treatment of an associated
338 neuropsychiatric disorder in FXS[22]. Notably, FXS is not the only neurological disorder
339 with overactive mTORC1. Tuberous Sclerosis Complex and Alzheimer's Disease both
340 have comorbid MDD and are reported to have overactive mTORC1 signaling[49-51]. While
341 NMDAR antagonists certainly have revolutionized the treatment of MDD in a general
342 population, caution should be exercised when utilizing them to treat individuals with
343 MDD and mTORC1-related diseases.

344

345 **Acknowledgments**

346 We thank Emma K. Erickson for generating preliminary data associated with this project
347 and Farr Niere for his valuable comments and suggestions. **Funding:** CFH (NIH/NIAAA
348 T32 AA007565), KRG (NSF IOS 1026527 NIH R01 AA026551, NIH P50 AA025117,

DoD USAMRMC W81XWH-14-1-0061). **Author contributions:** KRG, CFH, and SVN designed the studies; CFH, SVN, AU, and ECB, performed the experiments; KRG, CFH, and SVN performed analyses; KRG, JLW, CFH, and SVN wrote and edited the manuscript. **Competing interests**: The authors declare no competing interests. **Data and materials availability:** Sequencing data available in the NCBI Sequencing Read Archive (SRA) under submission SUB5029763. Code for RNAseq analysis available at https://github.com/snamjoshi.

Added note of proof: Since the original submission of this manuscript a recent report utilizes the same PLA assay to detect changes in synapse number.[52]

Supplementary information is available at MP's website.

361 **References**

362 1 Wei Y, Chang L, Hashimoto K. A historical review of antidepressant effects of
363 ketamine and its enantiomers. *Pharmacol Biochem Behav* 2020; **190**: 172870.

364 2 Li N, Lee B, Liu R-J, Banasr M, Dwyer JM, Iwata M *et al.* mTOR-dependent
365 synapse formation underlies the rapid antidepressant effects of NMDA antagonists.
366 *Science* 2010; **329**: 959–964.

367 3 Duman RS, Li N, Liu R-J, Duric V, Aghajanian GK. Signaling pathways underlying
368 the rapid antidepressant actions of ketamine. *Neuropharmacology* 2011; **62**: 35–41.

369 4 Trullas R, Folio T, Young A, Miller R, Boje K, Skolnick P. 1-
370 Aminocyclopropanecarboxylates exhibit antidepressant and anxiolytic actions in
371 animal models. *Eur J Pharmacol* 1991; **203**: 379–385.

372 5 Murrough JW, Iacoviello B, Neumeister A, Charney DS, Iosifescu DV. Cognitive
373 dysfunction in depression: neurocircuitry and new therapeutic strategies. *Neurobiol*
374 *Learn Mem* 2011; **96**: 553–563.

375 6 Duman RS. Ketamine and rapid-acting antidepressants: a new era in the battle
376 against depression and suicide. *F1000Res* 2018; **7**.
377 doi:10.12688/f1000research.14344.1.

378 7 Krystal JH, Abdallah CG, Sanacora G, Charney DS, Duman RS. Ketamine: A
379 Paradigm Shift for Depression Research and Treatment. *Neuron* 2019; **101**: 774–
380 778.

381 8 Workman ER, Niere F, Raab-Graham KF. Engaging homeostatic plasticity to treat
382 depression. *Mol Psychiatry* 2017; **23**: mp2017225–35.

383 9 Kiebler MA, Bassell GJ. Neuronal RNA granules: movers and makers. *Neuron*
384 2006; **51**: 685–690.

385 10 Lenzken SC, Achsel T, Carrì MT, Barabino SML. Neuronal RNA-binding proteins in
386 health and disease. *Wiley Interdiscip Rev RNA* 2014; **5**: 565–576.

387 11 Wolfe SA, Workman ER, Heaney CF, Niere F, Namjoshi S, Cacheaux LP *et al.*
388 FMRP regulates an ethanol-dependent shift in GABABR function and expression
389 with rapid antidepressant properties. *Nat Commun* 2016; **7**: 12867.

390 12 Dictenberg JB, Swanger SA, Antar LN, Singer RH, Bassell GJ. A direct role for
391 FMRP in activity-dependent dendritic mRNA transport links filopodial-spine
392 morphogenesis to fragile X syndrome. *Dev Cell* 2008; **14**: 926–939.

393 13 Darnell JC, Klann E. The translation of translational control by FMRP: therapeutic
394 targets for FXS. *Nat Neurosci* 2013; **16**: 1530–1536.

395 14 Abbeduto L, McDuffie A, Thurman AJ. The fragile X syndrome–autism comorbidity:
396 what do we really know? *Front Genet* 2014; **5**. doi:10.3389/fgene.2014.00355.

397 15 Hagerman R, Hoem G, Hagerman P. Fragile X and autism: Intertwined at the
398 molecular level leading to targeted treatments. *Mol Autism* 2010; **1**: 12.

399 16 Lugenbeel KA, Peier AM, Carson NL, Chudley AE, Nelson DL. Intragenic loss of
400 function mutations demonstrate the primary role of FMR1 in fragile X syndrome.
401 *Nat Genet* 1995; **10**: 483–485.

402 17 Roberts JE, Bailey DB, Mankowski J, Ford A, Sideris J, Weisenfeld LA *et al.* Mood
403 and anxiety disorders in females with the FMR1 premutation. *Am J Med Genet B*
404 *Neuropsychiatr Genet* 2009; **150B**: 130–139.

405 18 Johnston C, Eliez S, Dyer-Friedman J, Hessl D, Glaser B, Blasey C *et al.*
406 Neurobehavioral phenotype in carriers of the fragile X premutation. *American*
407 *Journal of Medical Genetics* 2001; **103**: 314–319.

408 19 Bourgeois JA, Seritan AL, Casillas EM, Hessl D, Schneider A, Yang Y *et al.*
409 Lifetime prevalence of mood and anxiety disorders in fragile X premutation carriers.
410 *J Clin Psychiatry* 2011; **72**: 175–182.

411 20 Kirsch AC, Huebner ARS, Mehta SQ, Howie FR, Weaver AL, Myers SM *et al.*
412 Association of Comorbid Mood and Anxiety Disorders With Autism Spectrum
413 Disorder. *JAMA Pediatr* 2019. doi:10.1001/jamapediatrics.2019.4368.

414 21 Weber JD, Smith E, Berry-Kravis E, Cadavid D, Hessl D, Erickson C. Voice of
415 People with Fragile X Syndrome and Their Families: Reports from a Survey on
416 Treatment Priorities. *Brain Sci* 2019; **9**. doi:10.3390/brainsci9020018.

417 22 The Lancet Neurology. A plan for fragile X syndrome with wide-ranging
418 consequences. *Lancet Neurol* 2019; **18**: 709.

419 23 Uutela M, Lindholm J, Rantamäki T, Umemori J, Hunter K, Võikar V *et al.*
420 Distinctive behavioral and cellular responses to fluoxetine in the mouse model for
421 Fragile X syndrome. *Front Cell Neurosci* 2014; **8**: 150.

422 24 Keene JD, Komisarow JM, Friedersdorf MB. RIP-Chip: the isolation and
423 identification of mRNAs, microRNAs and protein components of ribonucleoprotein
424 complexes from cell extracts. *Nat Protoc* 2006; **1**: 302–307.

425 25 Jain R, Devine T, George AD, Chittur SV, Baroni TE, Penalva LO *et al.* RIP-Chip
426 analysis: RNA-Binding Protein Immunoprecipitation-Microarray (Chip) Profiling.
427 *Methods Mol Biol* 2011; **703**: 247–263.

428 26 Workman ER, Niere F, Raab-Graham KF. mTORC1-dependent protein synthesis
429 underlying rapid antidepressant effect requires GABABR signaling.
430 *Neuropharmacology* 2013; **73**: 192–203.

431 27 Workman ER, Haddick PCG, Bush K, Dilly GA, Niere F, Zemelman BV *et al.* Rapid
432 antidepressants stimulate the decoupling of GABA(B) receptors from GIRK/Kir3
433 channels through increased protein stability of 14-3-3η. *Mol Psychiatry* 2015; **20**:
434 298–310.

435 28 Niere F, Namjoshi S, Song E, Dilly GA, Schoenhard G, Zemelman BV *et al.*
436 Analysis of Proteins That Rapidly Change Upon Mechanistic/Mammalian Target of
437 Rapamycin Complex 1 (mTORC1) Repression Identifies Parkinson Protein 7
438 (PARK7) as a Novel Protein Aberrantly Expressed in Tuberous Sclerosis Complex
439 (TSC). *Mol Cell Proteomics* 2016; **15**: 426–444.

440 29 Santarelli L, Saxe M, Gross C, Surget A, Battaglia F, Dulawa S *et al.* Requirement
441 of hippocampal neurogenesis for the behavioral effects of antidepressants. *Science*
442 2003; **301**: 805–809.

443 30 Brachman RA, McGowan JC, Perusini JN, Lim SC, Pham TH, Faye C *et al.*
444 Ketamine as a Prophylactic Against Stress-Induced Depressive-like Behavior. *Biol*
445 *Psychiatry* 2016; **79**: 776–786.

446 31 Surget A, Saxe M, Leman S, Ibarguen-Vargas Y, Chalon S, Griebel G *et al.* Drug-
447 dependent requirement of hippocampal neurogenesis in a model of depression and
448 of antidepressant reversal. *Biol Psychiatry* 2008; **64**: 293–301.

449 32 Li N, Liu R-J, Dwyer JM, Banasr M, Lee B, Son H *et al.* Glutamate N-methyl-D-
450 aspartate receptor antagonists rapidly reverse behavioral and synaptic deficits
451 caused by chronic stress exposure. *Biol Psychiatry* 2011; **69**: 754–761.

452 33 Darnell JC, Van Driesche SJ, Zhang C, Hung KYS, Mele A, Fraser CE *et al.* FMRP
453 stalls ribosomal translocation on mRNAs linked to synaptic function and autism.
454 *Cell* 2011; **146**: 247–261.

455 34 Law CW, Chen Y, Shi W, Smyth GK. voom: Precision weights unlock linear model
456 analysis tools for RNA-seq read counts. *Genome Biol* 2014; **15**: R29.

457 35 Antar LN, Bassell GJ. Sunrise at the synapse: the FMRP mRNP shaping the
458 synaptic interface. *Neuron* 2003; **37**: 555–558.

459 36 Südhof TC. Towards an Understanding of Synapse Formation. *Neuron* 2018; **100**:
460 276–293.

461 37 Micheva KD, Busse B, Weiler NC, O'Rourke N, Smith SJ. Single-synapse analysis
462 of a diverse synapse population: proteomic imaging methods and markers. *Neuron*
463 2010; **68**: 639–653.

464 38 Benson DL, Watkins FH, Steward O, Banker G. Characterization of GABAergic
465 neurons in hippocampal cell cultures. *J Neurocytol* 1994; **23**: 279–295.

466 39 De Simoni A, Griesinger CB, Edwards FA. Development of Rat CA1 Neurones in
467 Acute Versus Organotypic Slices: Role of Experience in Synaptic Morphology and
468 Activity. *The Journal of Physiology* 2003; **550**: 135–147.

469 40 Chowdhury GMI, Zhang J, Thomas M, Banasr M, Ma X, Pittman B *et al.* Transiently
470 increased glutamate cycling in rat PFC is associated with rapid onset of
471 antidepressant-like effects. *Mol Psychiatry* 2017; **22**: 120–126.

472 41 Berry-Kravis EM, Hessl D, Rathmell B, Zarevics P, Cherubini M, Walton-Bowen K
473 *et al.* Effects of STX209 (arbaclofen) on neurobehavioral function in children and
474 adults with fragile X syndrome: a randomized, controlled, phase 2 trial. *Science*
475 *Translational Medicine* 2012; **4**: 152ra127–152ra127.

476 42 Berry-Kravis E, Hagerman R, Visootsak J, Budimirovic D, Kaufmann WE, Cherubini
477 M *et al.* Arbaclofen in fragile X syndrome: results of phase 3 trials. *J Neurodev*
478 *Disord* 2017; **9**: 3.

479 43 Erickson CA, Veenstra-Vanderweele JM, Melmed RD, McCracken JT, Ginsberg
480 LD, Sikich L *et al.* STX209 (arbaclofen) for autism spectrum disorders: an 8-week
481 open-label study. *J Autism Dev Disord* 2014; **44**: 958–964.

482 44 Henderson C, Wijetunge L, Kinoshita MN, Shumway M, Hammond RS, Postma FR
483 *et al.* Reversal of disease-related pathologies in the fragile X mouse model by
484 selective activation of GABAB receptors with arbaclofen. *Science Translational*
485 *Medicine* 2012; **4**: 152ra128–152ra128.

486 45 Sinclair D, Featherstone R, Naschek M, Nam J, Du A, Wright S *et al.* GABA-B
487 Agonist Baclofen Normalizes Auditory-Evoked Neural Oscillations and Behavioral
488 Deficits in the Fmr1 Knockout Mouse Model of Fragile X Syndrome. *eNeuro* 2017;
489 **4**: ENEURO.0380–16.2017.

490 46 Zeidler S, Pop AS, Jaafar IA, de Boer H, Buijsen RAM, de Esch CEF *et al.*
491 Paradoxical effect of baclofen on social behavior in the fragile X syndrome mouse
492 model. *Brain Behav* 2018; **59**: e00991.

493 47 Wahlstrom-Helgren S, Klyachko VA. GABAB receptor-mediated feed-forward circuit
494 dysfunction in the mouse model of fragile X syndrome. *The Journal of Physiology*
495 2015; **593**: 5009–5024.

496 48 Abdallah CG, Averill LA, Gueorguieva R, Goktas S, Purohit P, Ranganathan M *et*
497 *al.* Modulation of the antidepressant effects of ketamine by the mTORC1 inhibitor
498 rapamycin. *Neuropsychopharmacology* 2020; **45**: 990–997.

499 49 Curatolo P, Moavero R, de Vries PJ. Neurological and neuropsychiatric aspects of
500 tuberous sclerosis complex. *Lancet Neurol* 2015; **14**: 733–745.

501 50 Rapp MA, Schnaider-Beeri M, Purohit DP, Perl DP, Haroutunian V, Sano M.
502 Increased neurofibrillary tangles in patients with Alzheimer disease with comorbid
503 depression. *Am J Geriatr Psychiatry* 2008; **16**: 168–174.

504 51 Li X, Alafuzoff I, Soininen H, Winblad B, Pei J-J. Levels of mTOR and its
505 downstream targets 4E-BP1, eEF2, and eEF2 kinase in relationships with tau in
506 Alzheimer's disease brain. *FEBS J* 2005; **272**: 4211–4220.

507 52 Dore K, Pao Y, Soria Lopez J, Aronson S, Zhan H, Ghosh S *et al.* SYNPLA, a
508 method to identify synapses displaying plasticity after learning. *Proc Natl Acad Sci*
509 *U S A* 2020; **117**: 3214–3219.

510 Figure Legends

511 **Figure 1.** ***The rapid antidepressant behavioral effects of Ro-25-6981 require FMRP***
512 ***expression.*** **A.** Representative timeline of behavioral procedures. Twenty-four hours
513 prior to the recorded forced swim test (FST), animals were acutely stressed with FST.
514 Approximately 22 hours later, animals received a single i.p. injection of their randomly
515 assigned treatment. Forty-five minutes after the injection, animals underwent the splash
516 test, and 30 minutes after that, they were exposed to a second FST. **B.** WT animals
517 treated with Ro-25-6981 significantly decreased the amount of time spent immobile in
518 the forced swim test, but *Fmr1* KO mice did not respond to treatment. Two-way ANOVA
519 revealed a significant main effect of treatment ($F_{1,41}$=7.023, p=0.0114) but did not find a
520 significant effect of genotype or genotype X treatment interaction. Newman-Keuls post-
521 hoc revealed a significant difference between WT control (170.8±10.3 s) vs. WT Ro-25-
522 6981 (109.4±14.8 s, n=17), but no significant difference between KO control
523 (131.3±20.0 s, n=7) and KO Ro-25-6981 (102.6±20.6 s, n=7). **C.** Similarly, Ro-25-6981-
524 treated WT animals increased their grooming frequency but treated *Fmr1* KO mice did
525 not. Two-way ANOVA revealed a significant main effect of treatment ($F_{1,46}$=4.314,
526 p=0.0434) and genotype ($F_{1,46}$=8.674, p=0.0051), but there was not a significant
527 genotype X treatment interaction. Newman-Keuls post-hoc revealed a significant
528 difference between WT control (1.92±0.32 times per minute, n=13;) vs. WT Ro-25-6981
529 (4.56±1.06 times per minute, n=16), but no significant difference between KO control
530 (1.00±0.43 times per minute) and KO Ro-25-6981 (1.42±0.48 times per minute, n=7).
531 Bars represent mean±SEM. *=p<0.05, **=p<0.01, n.s.=not significant.

532

533 **Figure 2**. ***mTORC1-sensitive FMRP-target mRNAs are regulated by Ro-25-6981***
534 ***treatment.*** **A.** *Top:* Venn diagram of differentially expressed mRNAs isolated in
535 Control/Ro-25-6981 or Ro-25-6981+Rapamycin/Ro-25-6981 conditions with the FDR
536 cutoff of 0.1 (same mRNAs as in Fig. 2B). *Bottom*: Breakdown of $\log_2$ fold-change
537 direction of mRNAs in the intersection of the Venn diagram, indicative of the mRNAs
538 that are sensitive to both treatment of Ro-25-6981 and mTORC1 activity. See Tables S4
539 and S5 for a complete list of genes and fold-changes. The single mRNA that is
540 oppositely regulated is Dbp, a transcription factor implicated in regulating circadian
541 rhythm. **B.** Clustered dendrogram and heatmap for $\log_2$ fold-change for the treatments.
542 Targets are the same as those in the pie chart in Fig. 2A. Dendrogram created using the
543 average linkage method and Euclidean distance metric. Positive fold-changes indicate
544 mRNAs are released from FMRP and presumably translated with Ro-25-6981
545 treatment; negative fold-changes indicate that more mRNAs are bound to FMRP with
546 Ro-25-6981 treatment compared to the control (indicative of mRNA repression with Ro-
547 25-6981 treatment) or Ro+Rapa (indicative that mTORC1 activity is needed for mRNAs
548 to be released with Ro-25-6981 treatment) conditions. **C.** In both Control/Ro-25-6981
549 and Ro-25-6981+Rapamycin/Ro-25-6981 conditions, *Fmr1* has a negative fold-change,
550 indicating that *Fmr1* mRNA remains bound to FMRP with Ro-25-6981 treatment and is
551 mTORC1 sensitive. Significance determined with the FDR cutoff of 0.1. **D.** Verification
552 that protein expression of FMRP decreases with Ro-25-6981 treatment in cortical
553 lysates 45 minutes after treatment, in line with previous reports[11] (control=1.0±0.03
554 normalized optical density, n=8; Ro-25-6981=0.83±0.07, n=8; t_{14}=2.008, p=0.0322). **E,**
555 **F.** Verification that protein expression of FMRP decreases with Ro-25-6981 treatment in

556 CA1 stratum radiatum 45 minutes after treatment (control=1.0±0.10 normalized optical
557 density, n=3; Ro-25-6981=0.69±0.05, n=9; t_{10}=2.717, *p*=0.0108). Bars represent
558 mean±SEM. *=*p*<0.05
559

560 **Figure 3.** ***FMRP-target mRNAs regulate transsynaptic signaling.*** **A.** Uniquely
561 enriched GO biological process clusters for FMRP targets identified by RIP-Seq where
562 $\log_2$(Control/Ro-25-6981 fold-change) > 0 (*blue)* and **B** $\log_2$(Ro-25-6981+Rapa/Ro-25-
563 6981 fold-change) > 0 (*pink*). Transsynaptic signaling is the most significantly enriched
564 GO cluster in both conditions. **C.** Scatterplot showing $\log_2$(Control/Ro-25-6981 fold-
565 change) > 0 $\log_2$(Ro-25-6981+Rapa/Ro-25-6981 fold-change) > 0 of the mTORC1-
566 sensitive transsynaptic targets (*upper right quadrant*). Supplemental Tables S4 and S5
567 contain the complete list of identified targets.
568

569 **Figure 4**. ***Transsynaptic signaling requires both NMDAR blockade and GABA$_B$R-***
570 ***mediated mTORC1 activation.*** **A.** Timeline of treatments for neuronal culture
571 experiments in 4B and 4F. **B.** Representative immunofluorescence images of treated
572 WT hippocampal neurons stained for PSD-95 (green), synapsin-1 (red), and MAP2
573 (grey outline). Panels depict 12.5 µm segments of dendrites, at least 20 µm from the
574 soma; scale bar=2 µm. Highlighted boxes indicate representative synapsin-1 and PSD-
575 95 staining; scale bar=0.5 µm. **C.** Quantification of average number of PSD-95 puncta
576 within dendritic area by treatment. PSD-95 expression increased in all treatments in an
577 mTORC1-independent manner. One-way ANOVA revealed a significant main effect of
578 treatment ($F_{3,65}$=6.472, *p*=0.0007). Newman-Keuls post-hoc revealed a significant

579 difference between control (1.0±0.18 normalized optical density, n=16) vs. Ro-25-6981
580 (2.02±0.33 normalized optical density, n=18), control vs. Ro-25-6981+Baclofen
581 (2.64±0.26 normalized optical density, n=18), and control vs. Ro-25-
582 6981+Rapamycin+Baclofen (2.75±0.40 normalized optical density, n=17). **D.**
583 Quantification of average number of synapsin-1 puncta within dendritic area by
584 treatment. One-way ANOVA revealed a significant main effect of treatment ($F_{3,65}$=15.31,
585 p<0.0001). Newman-Keuls post-hoc revealed Ro-25-6981+Baclofen (2.41±0.16
586 normalized optical density, n=18) significantly increased the number of synapsin-1
587 puncta compared to control-treated neurons (1.0±0.19 normalized optical density,
588 n=16), as well as neurons treated with Ro-25-6981 (0.91±0.17 normalized optical
589 density, n=18) and Ro-25-6981+Rapamycin+Baclofen (1.39±0.17 normalized optical
590 density, n=17), indicating an mTORC1-dependent effect. **E.** Quantification of Pearson's
591 correlation coefficient of PSD-95 and synapsin-1 by treatment. One-way ANOVA did not
592 reveal a significant effect of treatment for the correlation between PSD-95 and
593 synapsin-1 (control=0.15±0.03, n=16; Ro-25-6981=0.13±0.03, n=18; Ro-25-
594 6981+Baclofen=0.23±0.02, n=18; Ro-25-6981+Rapamycin+Baclofen=0.19±0.02, n=17).
595 **F.** Representative dendritic traces of treated hippocampal neurons. White puncta
596 represent proximity-detected PSD-95 and synapsin-1 proteins by PLA, and grey outline
597 represents MAP2 staining of the neuron. Puncta at least 12.5 μm from the soma were
598 analyzed. Scale bar for representative dendrites=10 μm. **G.** Quantification of the
599 average number of PSD-95/synapsin-1 PLA puncta per dendritic area. One-way
600 ANOVA revealed a significant main effect of treatment ($F_{4,581}$=18.25, p<0.0001).
601 Newman-Keuls post-hoc revealed Ro-25-6981+Baclofen (1.65±0.11 puncta/μm^2

602 normalized, n=132) significantly increased the number of PSD-95/synapsin-1 PLA
603 puncta compared to control-treated (1.0±0.10 puncta/μm^2 normalized, n=119), Ro-25-
604 6981-treated (1.12±0.84 puncta/μm^2 normalized, n=125), and Ro-
605 2506981+Rapamycin+Baclofen-treated (1.06±0.10 puncta/μm^2 normalized, n=143)
606 neurons. Additionally, PLA control neurons (0.05±0.01 puncta/μm^2 normalized, n=67)
607 showed a significant lack of puncta compared to all other treatments. **H.** Representative
608 PLA images indicating an increase in PSD-95/synapsin-1 PLA puncta in WT CA1
609 stratum radiatum 45 minutes after treatment with Ro-25-6981 and is blocked with the
610 $GABA_BR$ antagonist CGP35348; scale bar=50 μm. Bars represent mean±SEM.
611 *=p<0.05, **=p<0.01, ***=p<0.001, ****=p<0.0001, n.s.=not significant.
612
613 **Figure 5. *$GABA_BR$ activity is detrimental to synapse formation and rapid***
614 ***antidepressant efficacy of Ro-25-6981 in a preclinical mouse model of FXS.* A.**
615 Representative PLA images in KO CA1 stratum radiatum 45 minutes after treatment;
616 scale bar=50 μm. **B.** Quantification of the average number of PSD-95/synapsin-1 PLA
617 puncta per CA1 stratum radiatum area. One-way ANOVA revealed a significant main
618 effect of treatment ($F_{2,10}$=25.45, p=0.0001). Newman-Keuls post-hoc revealed Ro-25-
619 6981 (0.57±0.02 puncta/μm^2 normalized, n=4) significantly decreases PLA puncta
620 compared to control (1.0±0.09 puncta/μm^2 normalized, n=4), but blocking $GABA_BRs$
621 with CGP35348 increases the number of puncta (1.47±0.10 puncta/μm^2 normalized,
622 n=5) compared to both other treatments. **C.** One-way ANOVA revealed a significant
623 main effect of treatment ($F_{2,17}$=4.23, p=0.0323) in the FST. Newman-Keuls post-hoc
624 revealed *Fmr1* KO animals treated with Ro-25-6981+CGP35348 (42.38±13.66 s, n=9)

625 significantly decrease immobility in the FST compared to control (111.5±9.2 s, n=6), but
626 not Ro-25-6981-treatment only (90.1±32.8 s, n=5). WT data from Figure 1 depicted on
627 the y-axis for reference. **D.** Similarly, one-way ANOVA revealed a significant main effect
628 of treatment ($F_{2,17}$=4.854, *p*=0.0215) in the splash test. Newman-Keuls post-hoc
629 revealed Ro-25-6981+CGP35348 (7.4±1.3 times per minute, n=10) significantly
630 increases grooming frequency in the splash test compared to control (1.4±0.4 times per
631 minute, n=5) but not Ro-25-6981-treatment only (5.2±1.5 times per minute, n=5) for
632 *Fmr1* KO animals. WT data from Figure 1 depicted on the y-axis for reference. **E.**
633 Updated rapid antidepressant signaling mechanism model[11,26,27] to include RIP-Seq
634 results. Under baseline conditions, activated NMDARs increase intracellular calcium,
635 which activates mTORC1 (*left panel*). With NMDAR antagonists like ketamine and Ro-
636 25-6981, NMDARs are blocked but activate the release or binding of mRNAs from the
637 RNA-binding protein FMRP (*middle panel*). Among these released transcripts is
638 $GABA_BR$ mRNA, which is translated into newly synthesize $GABA_BRs$[26]. Old $GABA_BRs$
639 and the GIRK channels they are coupled to undergo endocytosis[27]. Newly synthesized
640 $GABA_BRs$ are coupled to L-type calcium channels and, upon activation, increase
641 intracellular calcium, activating mTORC1 (*right panel*)[27]. mTORC1-dependent
642 transcripts are released from or bound to FMRP, including those mediating a
643 transsynaptic signal that recruits presynaptic engagement to help form new synapses.
644 Yellow boxes with stars indicate the new steps added to the model based on the current
645 data presented. Bars represent mean±SEM. *=*p*<0.05, **=*p*<0.01, ****=*p*<0.0001.

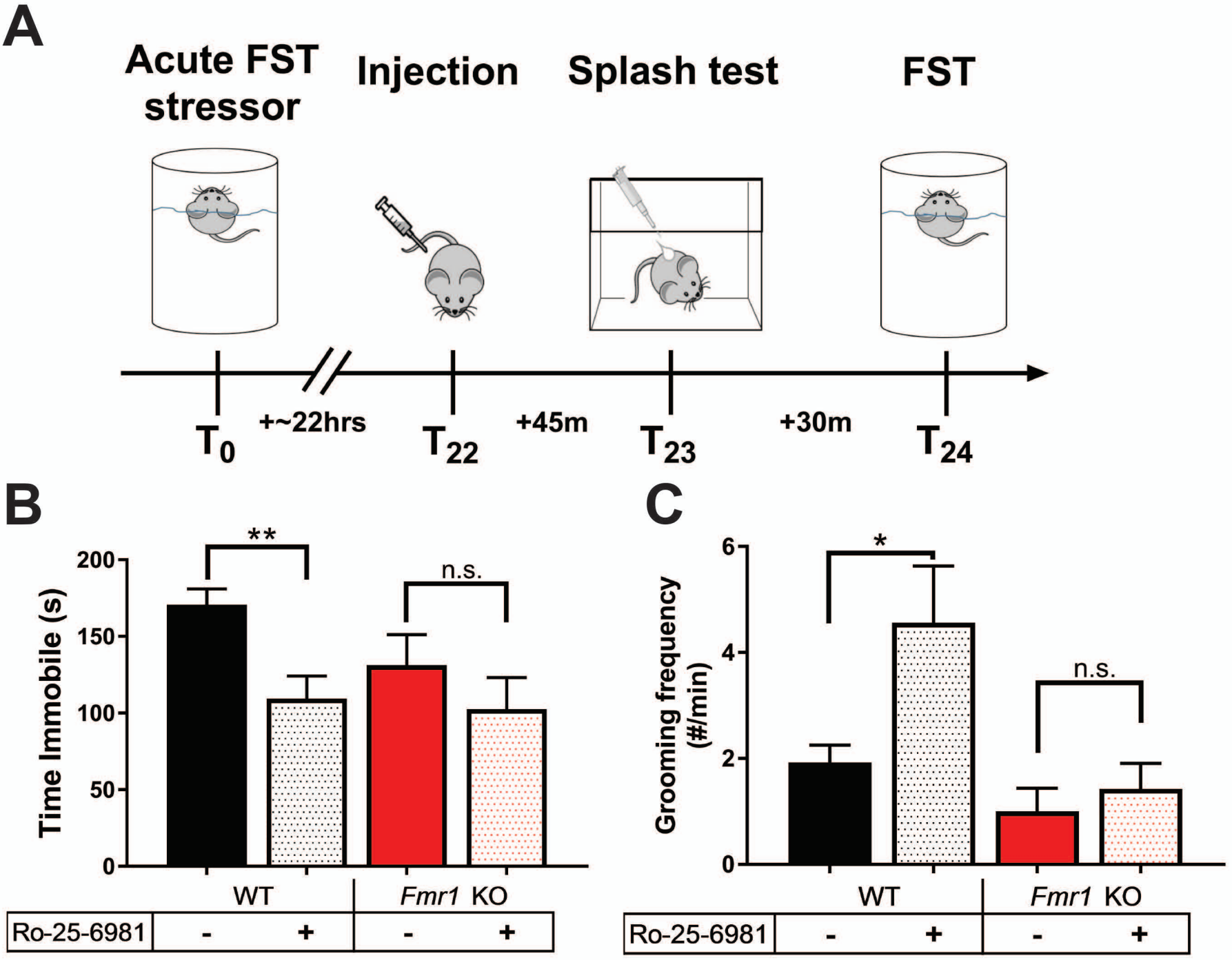
A
Acute FST stressor
Injection
Splash test
FST
T0
+~22hrs
T22
+45m
T23
+30m
T24
B
Time Immobile (s)
200
150
100
50
0
**
n.s.
WT
Fmr1 KO
Ro-25-6981
-
+
-
+
C
Grooming frequency (#/min)
6
4
2
0
*
n.s.
WT
Fmr1 KO
Ro-25-6981
-
+
-
+

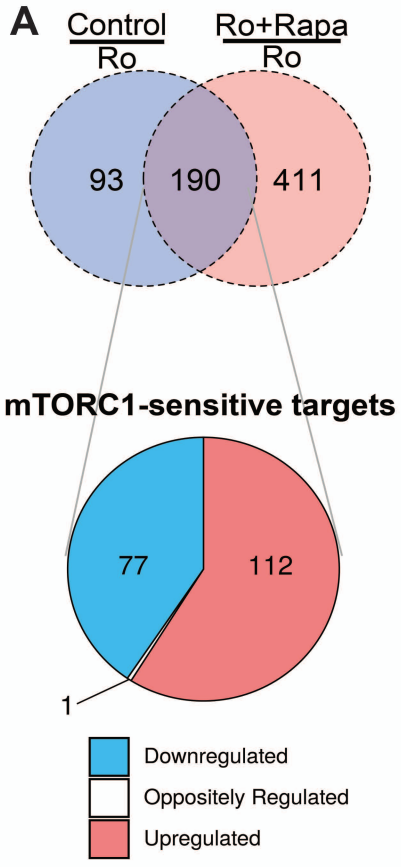

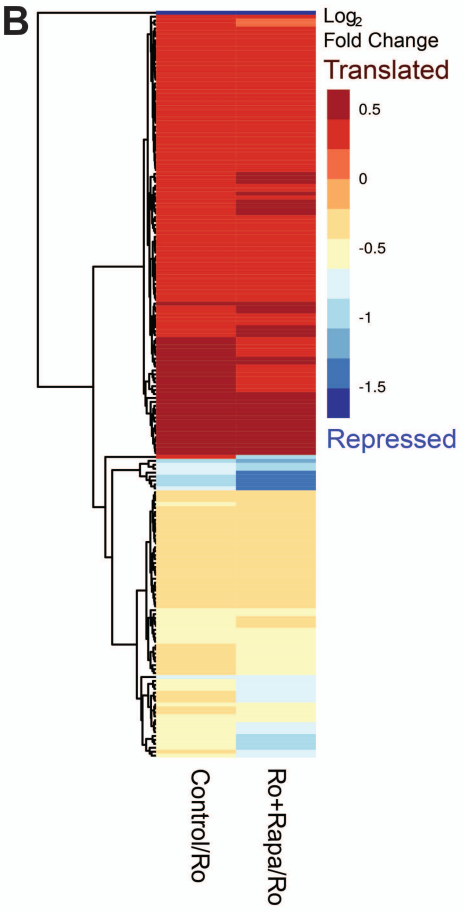

C

Fmr1	logFC	adj.P.Val
Control/Ro	-0.3093	0.0772
Ro+Rapa/Ro	-0.5727	0.0059

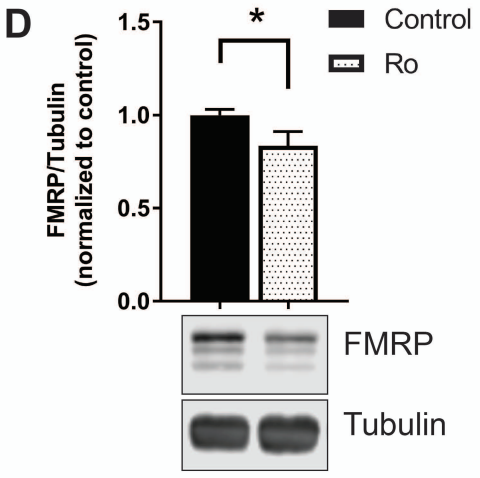

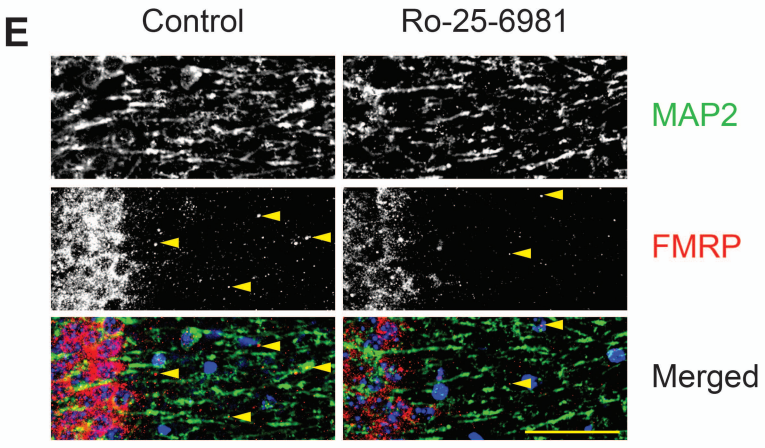

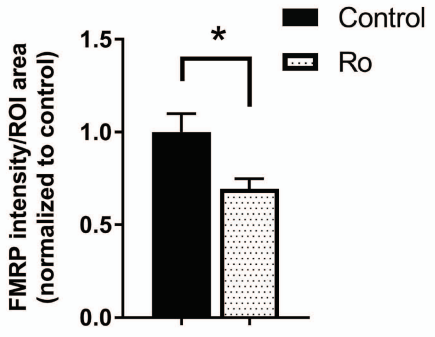

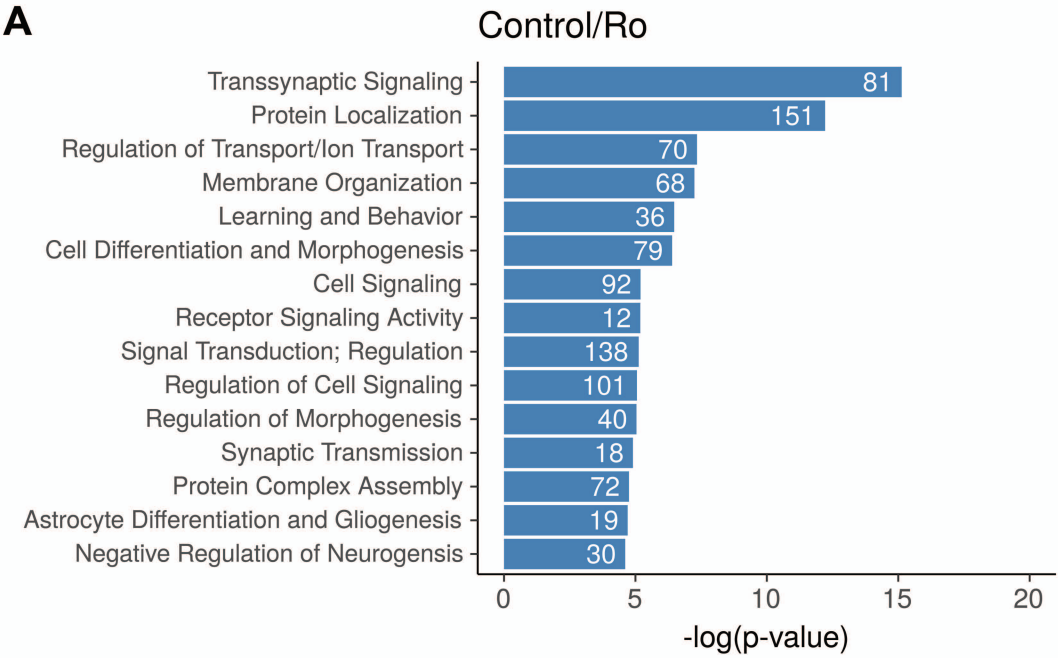
A
Control/Ro
Transsynaptic Signaling
Protein Localization
Regulation of Transport/Ion Transport
Membrane Organization
Learning and Behavior
Cell Differentiation and Morphogenesis
Cell Signaling
Receptor Signaling Activity
Signal Transduction; Regulation
Regulation of Cell Signaling
Regulation of Morphogenesis
Synaptic Transmission
Protein Complex Assembly
Astrocyte Differentiation and Gliogenesis
Negative Regulation of Neurogensis
81
151
70
68
36
79
92
12
138
101
40
18
72
19
30
0
5
10
15
20
-log(p-value)

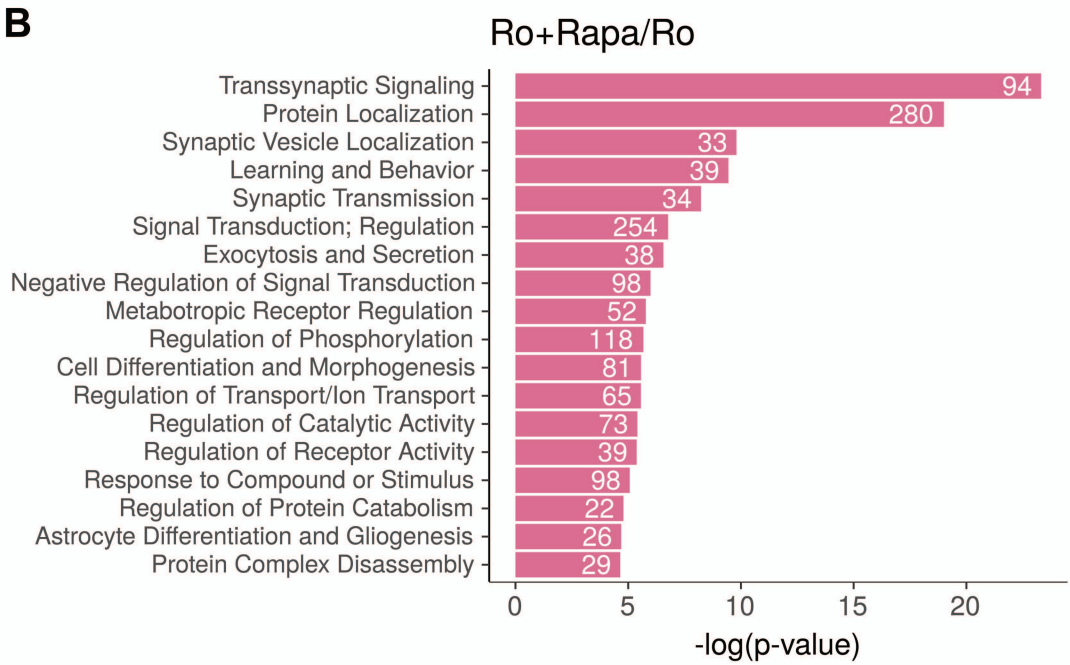
B
Ro+Rapa/Ro
Transsynaptic Signaling
Protein Localization
Synaptic Vesicle Localization
Learning and Behavior
Synaptic Transmission
Signal Transduction; Regulation
Exocytosis and Secretion
Negative Regulation of Signal Transduction
Metabotropic Receptor Regulation
Regulation of Phosphorylation
Cell Differentiation and Morphogenesis
Regulation of Transport/Ion Transport
Regulation of Catalytic Activity
Regulation of Receptor Activity
Response to Compound or Stimulus
Regulation of Protein Catabolism
Astrocyte Differentiation and Gliogenesis
Protein Complex Disassembly
94
280
33
39
34
254
38
98
52
118
81
65
73
39
98
22
26
29
0
5
10
15
20
-log(p-value)

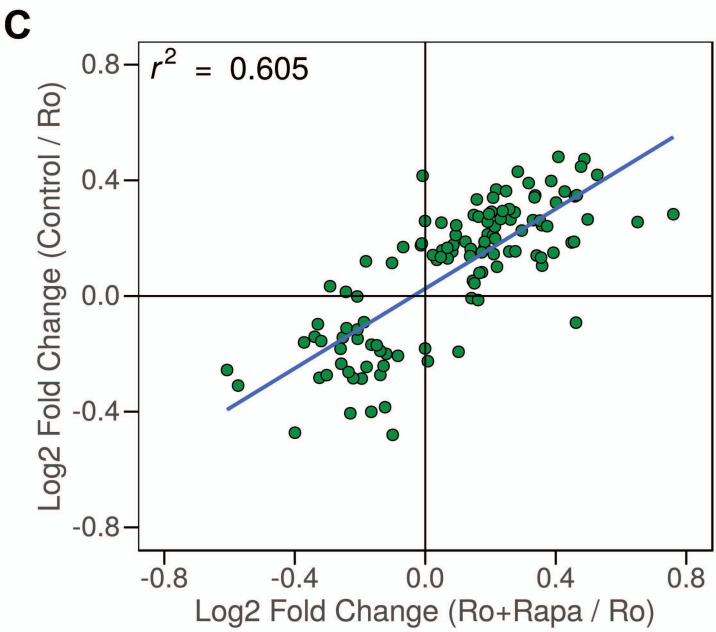
C
r^2 = 0.605
0.8
0.4
0.0
-0.4
-0.8
Log2 Fold Change (Control / Ro)
-0.8
-0.4
0.0
0.4
0.8
Log2 Fold Change (Ro+Rapa / Ro)

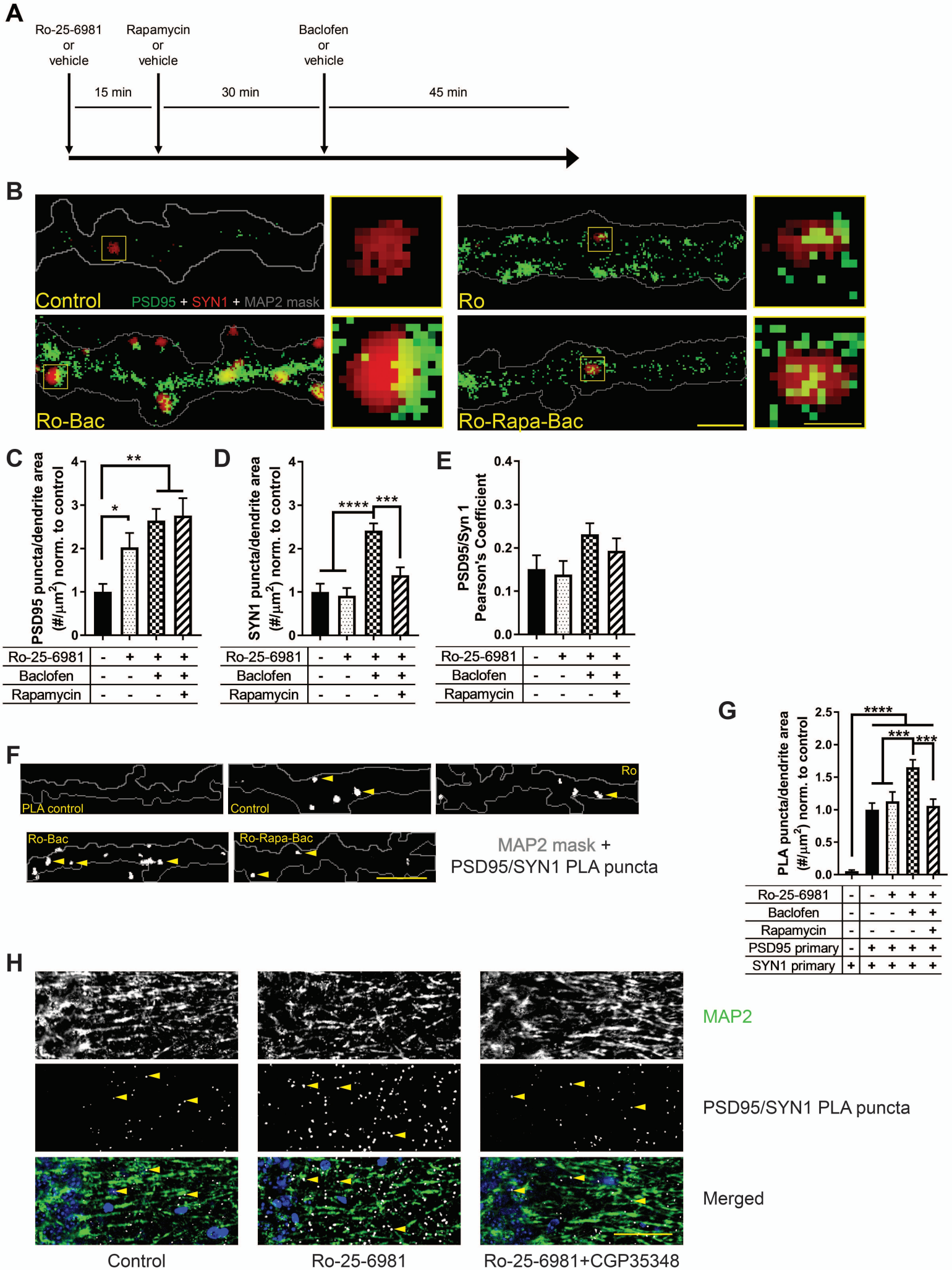
A
Ro-25-6981 or vehicle
Rapamycin or vehicle
Baclofen or vehicle
15 min
30 min
45 min
B
Control
PSD95 + SYN1 + MAP2 mask
Ro
Ro-Bac
Ro-Rapa-Bac
C
PSD95 puncta/dendrite area (#/μm2) norm. to control
D
SYN1 puncta/dendrite area (#/μm2) norm. to control
E
PSD95/Syn 1 Pearson's Coefficient
Ro-25-6981
Baclofen
Rapamycin
F
PLA control
Control
Ro
Ro-Bac
Ro-Rapa-Bac
MAP2 mask + PSD95/SYN1 PLA puncta
G
PLA puncta/dendrite area (#/μm2) norm. to control
PSD95 primary
SYN1 primary
H
MAP2
PSD95/SYN1 PLA puncta
Merged
Control
Ro-25-6981
Ro-25-6981+CGP35348

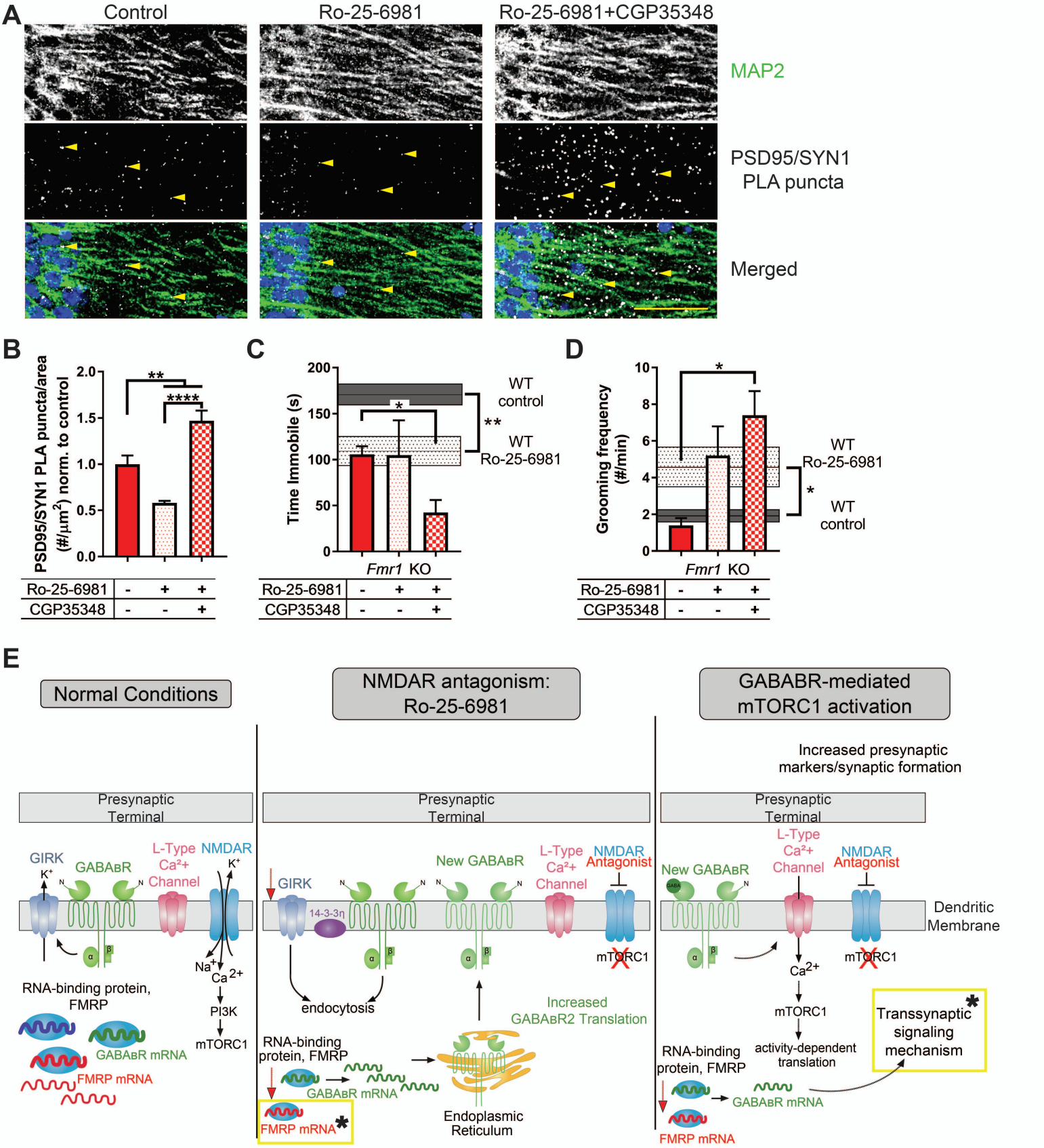
A
Control
Ro-25-6981
Ro-25-6981+CGP35348
MAP2
PSD95/SYN1
PLA puncta
Merged
B
PSD95/SYN1 PLA puncta/area (#/μm²) norm. to control
2.0
1.5
1.0
0.5
0.0
**
****
Ro-25-6981 - + +
CGP35348 - - +
C
Time Immobile (s)
200
150
100
50
0
*
**
WT control
WT Ro-25-6981
Fmr1 KO
Ro-25-6981 - + +
CGP35348 - - +
D
Grooming frequency (#/min)
10
8
6
4
2
0
*
*
WT Ro-25-6981
WT control
Fmr1 KO
Ro-25-6981 - + +
CGP35348 - - +
E
Normal Conditions
NMDAR antagonism: Ro-25-6981
GABABR-mediated mTORC1 activation
Increased presynaptic markers/synaptic formation
Presynaptic Terminal
Presynaptic Terminal
Presynaptic Terminal
GIRK
K+
GABABR
L-Type Ca2+ Channel
NMDAR
K+
Na+
Ca 2+
PI3K
mTORC1
RNA-binding protein, FMRP
GABABR mRNA
FMRP mRNA
GIRK
14-3-3η
New GABABR
L-Type Ca2+ Channel
NMDAR Antagonist
mTORC1
endocytosis
Increased GABABR2 Translation
RNA-binding protein, FMRP
GABABR mRNA
FMRP mRNA
Endoplasmic Reticulum
New GABABR
L-Type Ca2+ Channel
NMDAR Antagonist
Dendritic Membrane
Ca2+
mTORC1
mTORC1
activity-dependent translation
Transsynaptic signaling mechanism
RNA-binding protein, FMRP
GABABR mRNA
FMRP mRNA